An Improved DC-Link Voltage Control Strategy for Grid Connected Converters

Pranali Chopade[1], Prof. S. Sananse[2]

PG Student [EPS], Dept. of EE, KCES'S College of Engineering and IT, Jalgaon, Maharashtra, India[1]

Assistant Professor, Dept. of EE, KCES'S College of Engineering and IT, Jalgaon, Maharashtra, India[2]

ABSTRACT: This paper presents a robust control strategy to improve dc-link voltage control performances for Grid connected Converters (GcCs). The proposed control strategy is based on an adaptive PI controller and is aimed to ensure fast transient response, low dc-link voltage fluctuations, low grid current THD and good disturbance rejection after sudden changes of the active power drawn by the GcC. The proportional and integral gains of the considered adaptive PI controller are self-tuned so that they are well suited with regard to the operating point of the controlled system and/or its state. Several simulation and experimental results are presented to confirm and validate the effectiveness and feasibility of the proposed dc-link voltage control strategy.

KEYWORDS: DC-link voltage control, adaptive PI controller, Grid connected Converters

I. INTRODUCTION

Nowadays, power converters have an important role in a large scale of industrial applications since they allow efficient power transmission between the grid (on one side) and loads or energy sources (on the other side). The commonly used power converters topologies use a dc-link as an intermediate stage for the power conversion process in addition to a Grid connected Converter (GcC) and a filter based on passive (inductive and/or capacitive) elements. For example, this is the case of adjustable speed drives, renewable energy sources active power filters, UPS systems and back-to-back systems. Efficient dc-link voltage control is very important for such applications to reduce voltage fluctuations in the dc-link which are mainly caused by random changes (particularly sudden and sever changes) in the power drawn by the GcC. When these fluctuations cross their limits, the protection devices are activated leading to a system shut-down. Thus, the control objectives pertaining to the dc-link voltage can be summarized in the following key points: 1) the voltage across the dc-link capacitor must be kept at a constant value by controlling the power flow in the AC side of the GcC so that two objectives are satisfied: the first one is the upkeep of the capacitor charge, while the second one is the supply of a load connected to the dc-link (for the rectifying mode case) or the transfer of the power provided by a DC source (for the inverting mode case), 2) the dc-link voltage fluctuations must be minimized, 3) the generation of high grid current harmonics must be prevented and 4) The deviation from the unity power factor operation caused by the grid current ripples must be prevented. The most frequently used dc-link voltage controller is the PI controller Different PI controller design techniques were described in literature. Among them, we can cite the pole zero cancellation method, the pole placement method and the optimum criterion method. For these methods, the PI controller is usually adjusted with respect to different constraints: $C1$) stability; $C2$) dynamic performances; $C3$) disturbance rejection; and $C4$) step responses with low overshoot. In order to satisfy all these constraints, some research works presented the design of adaptive PI controllers. Other ones combine between the benefits of the PI controller and the feed forward compensation method. For that case, despite the excellent improvement of dynamic performances, such a method increases the coupling between the controlled dc-link voltage and the grid currents. Consequently, any noise or fast oscillation in the grid currents can create ripples at the output reference of the dc-link voltage controller. Other works have presented a Direct Power Control (DPC) combined with the boundary control to improve the dynamic performances of the dc-link voltage. Compared to the conventional DPC, the dc-link voltage is considered for selection of the switching states through a switching table. As a result, no outer loop is needed and the dynamic performances are highly improved. However, this method results into a variable switching frequency, which is limited to the half of the used sampling period and which depends on the system parameters, dc-link voltage and ac-side voltage. So, the DPC combined with boundary control cannot be used for applications that require constant switching frequency, like the case of LCL-based GcCs since it will lead to resonance problems. Moreover, this control will lead to high grid current THD values during steady state operation if low mean switching frequency is achieved.

## II.SYSTEM MODEL AND ASSUMPTIONS
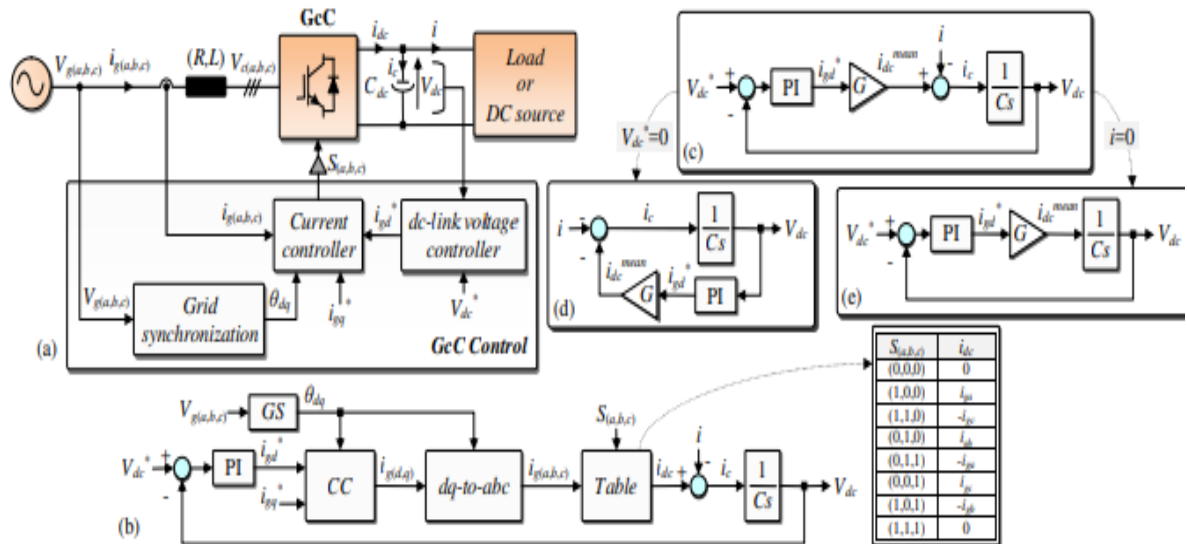
Fig. 1. (a) Commonly used control structure for Grid-connected Converters (b) Model of the dc-link voltage control system (c) Simplified model of the dc-link voltage control system (d) Equivalent simplified model when $Vdc^*=0$ (e) Equivalent simplified model when $i=0$

This paper proposes an efficient adaptive PI controller for the dc-link voltage control. The adaptive nature of the proposed PI controller guarantees the different control constraints $C(1..4)$ mentioned in the previous paragraph in addition to the reduction of grid current THD during steady state operation, which is mainly caused by dc-link voltage controller's output signal. The proportional and integral gains of the considered adaptive PI controller are self-tuned according to the operating point of the controlled system and/or its state (*i.e.* transient or steady state). For that, a band around the dc-link voltage reference is defined. When the measured dc-link voltage is outside this band, the PI gains were selected constants so that a very good dynamic is achieved. Otherwise, the PI gains become variable so that the previously mentioned constrains remain still satisfied. Also, an anti-windup process is added in order to prevent large overshoot after step jumps of the dc-link voltage reference. The rest of the paper is organized as follow. Section II presents a simplified modeling, analysis and design of the dc link voltage controller. Then, section III describes the proposed adaptive dc-link voltage controller. Accordingly, section IV shows and discusses the obtained experimental results with the proposed adaptive PI controller. Finally, section V summarizes the main conclusions of this work.

III. SYSTEM DESCRIPTION

Simulations are done in order to compare the performances of the adaptive PI controller (including the anti-wind-up action) with those of the standard PI controller. The used simulation parameters are depicted on Tab.1 and the obtained simulation results are shown on Fig.3. Fig.3.a compares between simulations results obtained with the standard PI control (for constant PI gains tuned for $\omega n=\omega n\min$ and $\omega n=\omega nopt$) and those obtained with the proposed adaptive PI control. The natural frequency $\omega nopt$ is determined so that, when a step jump equal to Imax is applied to the input current i, the resulting Mp value is equal to $GdcVdc^*=10\%Vdc^*$. So, based on equation (9), $\omega nopt$ is computed as follows

$$W_{nopt} = F_5(0.7) \frac{IMax}{Gdc\,Vdc^*} = \frac{416.88 \times 1.25}{0.1*150} = 34.74 \text{ rad/s}$$

It can be noted that the adaptive PI control ensures shorter transient time with lower drop of the dc-link voltage after a step jump (at $t=0.5$s) of the input current i equal to Imax.
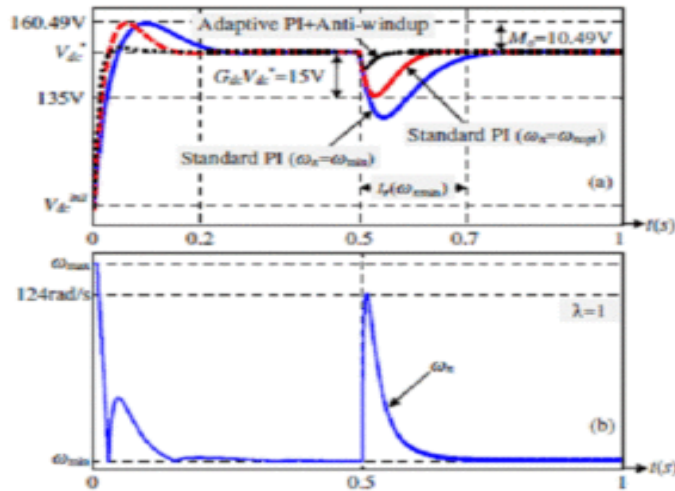
Fig. 3. Simulation results (ξ=0.7, *Vdc init*=100V, *Vdc* *=150, *i*=0 at *t*=0s and *i*=*I*max at *t*=0.5s) (a) Comparison between standard PI control and adaptive PI control (b) waveform of the selected ωn value for the adaptive PI controller

TABLE I
SYSTEM PARAMETERS

Symbol	Description	Value	Unit
S	GcC rated power	20	KVA
L	Industive filter	40	mH
C	Dc-Link Voltage capacitor	1100	µF
Z$_{load}$	Load Inpendance	120	Ω
I$_{max}$	Maximum load cureent	1.25	A
V$_{dc\ intl}$	Dc link Voltade initial value	100	V
V$_{dc}$	Dc link voltage Referance value	150	V
G$_{dc}$	Ratio of the DC-link voltage band	10	%
λ	Used coefficient for ω_n *computation*	1	-
ω_{nmax}	Maximum natural frequncy	$2\pi22.73$	rad/s
$\omega nopt$	Optimal natural Frequncy	$2\pi5.35$	rad/s
$\omega nmin$	Minimal natural Frequncy	$2\pi3.5$	rad/s
ξ	Damping ratio	0.7	-
K$_c$	Anti- windup coefficient	0.02	-
T$_s$	Sampling period	50	µs

Fig.3.b illustrates the waveform of the selected ωn value for the adaptive PI controller. Notice that ωn is almost equal to ωnmin during steady state operation. During transient states it increases considerably and becomes equal to $\omega nmax$ when the magnitude of the dc-link voltage error exceeds the band limit (during startup). It should be noted here that the maximum overshoot resulting from a step jump of the input current *I* equal to *I*max at *t*=0.5s is significantly lower for the case of an adaptive PI controller compared to the case of a standard PI controller with constant gains and tuned for $\omega n=\omega nopt$.c Moreover, as the selected ωn value used for updating the ($\check{K}pdc$, $\check{K}pdc$) gains of the adaptive PI controller increases rapidly when the magnitude of the dc-link voltage error increases, the obtained *Mp* value with the adaptive PI controller can be approximated to that obtained for a standard PI controller with constant gains tuned for $\omega n=\omega nmax$.

IV. EXPERIMENTAL RESULT

In order to verify the efficiency of the proposed controller, the prototyping platform presented on Fig. 4 was developed. It includes three parts. The first one is a power part, which is composed of: 1) a three-phase autotransformer used to impose the desired grid voltage peak magnitude; 2) a three-phase inductive filter *L*; 3) a three-phase GcC; 4) a DC-link capacitor *C*; and 5) a resistive load *ZLoad*. The second one is the control part composed of 1) the STM32F4-Discovery digital solution and 2) a Host PC. Note that the used digital solution is based on Cortex-M4-ARM processor, which is associated to a Floating Point Unit (FPU) and have a system clock frequency equal to 168 MHz. Finally, the third part is an interface part that includes:1) a measurement board used to acquire seven analog measurements (*Vg(a,b,c)*,

$ig(a,b,c)$ and *Vdc*) and 2) an interface board used to amplify the computed switching signals $S(a,b,c)$. The used parameters for the experimental tests are the same as the ones presented in Tab.1.

① Autotransformer ② Inductors ③ GcC ④ Scope ⑤ Host PC
⑥ Measurement board ⑦ Microcontroller ⑨ Resistive load
⑧ Switching signals interface board
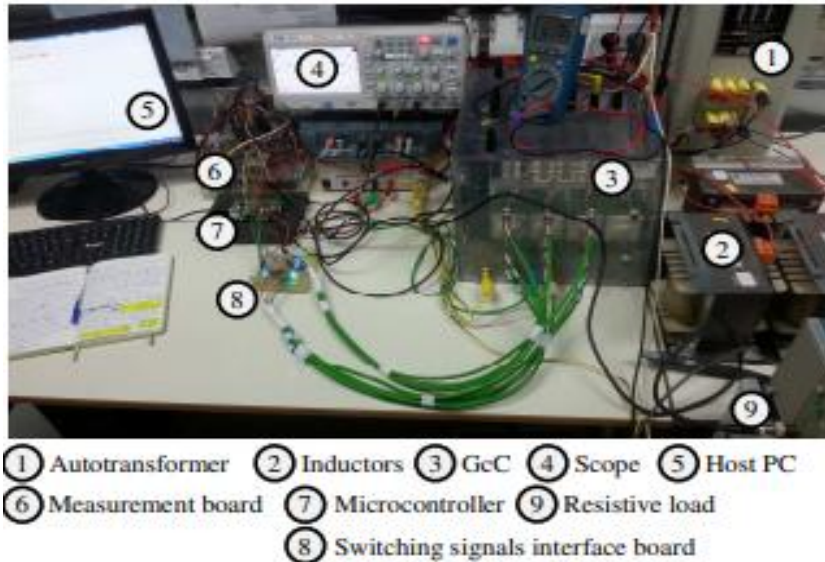
In order to eliminate noises in the measured dc-link voltage, equation (15) was implemented with a small modification. The selected $\omega n[k]$ value during a *kth* sampling period is computed by replacing $|\Delta Vdc[k]|$ in (15) by $|\Delta Vdc|min[k]$, which is equal to the minimal value of $(|\Delta Vdc(j)|j=(k-n+1\dots k)$ (n was set to 5 for efficient elimination of the noises). The experimental tests were done according to the following steps:

- Step 1: The GcC switching signals were all tied at a low logical level. For that case, the GcC works as a simple three phase diode bridge rectifier and the capacitor charge was initially set to 100V by acting on the ratio of the autotransformer. Also, the load *Zload* was disconnected.

- Step 2: The switching signals $S(a,b,c)$ were applied to the GcC and a step jump equal to 150V is applied to the dc-link voltage reference *Vdc**. The experimental results related to step 1 and 2 are presented in Fig.5.a, Fig.5.b and Fig.5.c. These figures compare between three cases: 1) a standard PI controller tuned for $\omega n=\omega n$min (Fig.5.a), 2) a standard PI controller tuned for $\omega n=\omega n opt$ (Fig.5.b) and 3) the proposed controller (Fig.5.c). It can be noted that the proposed controller ensures a dc-link voltage step response with good dynamic performances and without overshoot during the first transient states.

Step 3: As explained previously, the proposed method supposes that the input current will not exceed a predefined

maximum value Imax. The worst case that will lead to a maximum overshoot value Mp is a sudden and sever change of the input current i that can be approximated to a step jump from 0 to Imax (for a sudden maximum power load connection). For others kinds of loads, characterized by a smoother input current i change, the overshoot will be lower than the considered worst case. During step 3, the control performances in terms of disturbance rejection were tested through a sudden connection of a resistive load $ZLoad$ equal to $Vdc*/Imax$=150V/1.25A=120Ω. The experimental results related to steps 2 and 3 are presented in Fig.5.d, Fig.5.e and Fig.5.f.These figures compare between three cases: 1) a standard PI controller tuned for $\omega n=\omega n$min (Fig.5.d), 2) a standard PI controller tuned for $\omega n=\omega nopt$ (Fig.5.e) and 3) the proposed controller (Fig.5.f). It can be noticed that the input current I response can be approximated to a step jump from 0 to $Imax$ and that the obtained experimental results are quite close to those obtained in simulation results shown in Fig.3. Finally, Fig.6 shows the grid voltage Vga waveform with regard to the grid current iga and the estimated θdq position waveforms during steady state operation for a standard PI controller tuned for $\omega n=\omega nopt$ (Fig.6.a) and for the proposed adaptive PI controller (Fig.6.b). This figure shows that a unity power factor operation
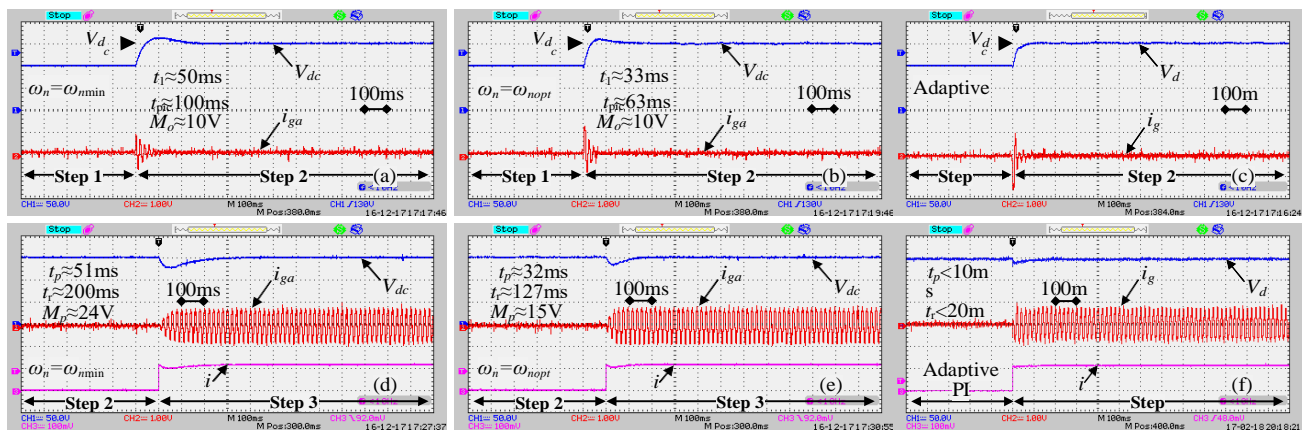
was achieved for both cases. Also, the use of the adaptive PI controller allowed the reduction of the grid current THD (the THD was reduced from 5.26% for the case of a standard PI controller to 4.12% for the proposed controller).

Fig. 5. (a-b-c) DC-link voltage V_{dc} (50V/div) and grid current i_{ga} (3.28A/div) waveforms during steps 1 and 2 (a) Standard PI controller ($\omega n=\omega n$min) (b) Standard PI controller ($\omega n=\omega nopt$) (c) Proposed adaptive PI controller (e-f-g) DC-link voltage V_{dc} (50V/div) and grid current i_{ga} (3.28A/div) waveforms during steps 2 and 3 (e) Standard PI controller ($\omega n=\omega n$min) (f) Standard PI controller ($\omega n=\omega nopt$) (g) Proposed adaptive PI controller

VI.CONCLUSION

This paper presented an improved dc-link voltage controller based on an adaptive PI controller with an anti windup process. The proportional and integral gains of the proposed PI controller are self-tuned so that the following constraints are satisfied: 1) no overshoot after step jumps of the dc-link voltage reference input; 2) fast dynamic response after step jumps of the dc-link voltage reference; 3) fast dynamic response after step jump of the input current i and 4) low grid current THD value during steady state operation. The considered control was experimentally tested on a prototyping platform. The obtained experimental results are quite similar to simulation results and show the effectiveness and reliability of the adopted control strategy.

REFERENCES

[1] D. Casadei, M. Mengoni, G. Serra, A. Tani, and L. Zarri, "A control scheme with energy saving and dc-link overvoltage rejection for induction motor drives of electric vehicles," IEEE Trans. Ind. Appl., vol. 46, no. 4, pp. 1436–1446, Jul./Aug. 2010.

[2] Li, F., Zou, Y.P., Wang, C.Z., Chen, W., Zhang, Y.C., Zhang, J., "Research on AC Electronic Load Based on back to back Single phase PWM Rectifiers," Applied Power Electronics Conference and Exposition, 2008. APEC 2008. Twenty-Third Annual IEEE. 2008, pp.630-634. 2008.

[3] M. Karimi-Ghartimani, S.A. Khajehoddin, P. Jain, A. Bakhshai, "A systematic approach to dc-bus control design in single phase grid connected renewable converters," IEEE Trans. Power Electron, vol. 28, no. 7, pp. 3158–3166, July. 2013.

[4] X. Yuan, F. Wang, D. Boroyevich, Y. Li, and R. Burgos, "Dc-link voltage control of a full power converter for wind generator operating.